

Analysis and Prediction of Process Parameters During Laser Deposition Manufacturing Based on Melt Pool Monitoring

Qin Lanyun, Xu Lili, Yang Guang, Shang Chun, Wang Wei

Key Laboratory of Fundamental Science for National Defense of Aeronautical Digital Manufacturing Process, Shenyang Aerospace University, Shenyang 110136, China

Abstract: During laser deposition manufacturing (LDM) process, melt pool width which is greatly influenced by process parameters is essential for the forming tracks geometry. In this paper, the melt pool geometry evolution was monitored by a CCD camera, and a method of applying Kalman filtering for the melt pool width detection during LDM process was presented to obtain accurate values. Orthogonal experimental design and multiple regression analysis were used to establish an empirical model describing the correlation between the melt pool width and three main process parameters (laser power, scanning speed, and powder feeding rate). And the developed model was verified experimentally. Finally, particle swarm optimization (PSO) was implemented for prediction of process parameters during the buildup of a thin wall. The results indicate that process parameters analysis and prediction for LDM process could make it possible to acquire an efficient process for the forming tracks geometry control.

Key words: laser deposition manufacturing; melt pool; particle swarm optimization; empirical model; Kalman filter

Laser deposition manufacturing (LDM) is a laser cladding based additive manufacturing (AM) technology, which shows wide application potentials in the areas of aerospace, automotives, and biomedical science, etc^[1-3]. LDM involves complicated interactions among laser, powder and melt pool^[4,5]. A laser is utilized as a heat source to melt powder particles and create a moving melt pool on the substrate. The solidification of powders caught by the melt pool leads to the fabrication of a part layer by layer. Compared to the conventional techniques, LDM has the ability to produce parts of various shapes with many distinct advantages such as superior mechanical properties, homogenous metallurgical bonding, and low dilution^[6-8]. Based on the rapid heating and cooling characteristics of laser material processing, LDM can greatly reduce production cost and cycle. With the growing economical expectations in industries, the demand for high quality parts in various industrial fields rises. However, a high quality part should meet the standards of high deposition precision, low dilution and minimal porosity. Moreover, the forming process is

of high sensitivity to the condition variation^[9,10], fluctuations in the process parameters (i.e., laser power, powder feeding rate, and scanning speed), deposition environment (i.e., temperature, humidity, and powder distribution), and deposition process (i.e., reflection of the melt pool, flow in the melt pool, and surface tension) will deflect the process from the pre-optimized condition, which would result in different degrees of forming defects and quality variations. The forming part is therefore prone to suffer from instability of the melt pool. As a result, online monitoring and accurately control of the deposition process are very challenging.

In order to meet the demanding requirements of the aerospace, automotive, rapid tooling and biomedical sectors, problems that the LDM faced such as the optimization of micro-structure, the size control of forming parts and the improvement of forming process efficiency are still needed to be solved. To ensure quality and geometry precision of the forming part, many researchers have studied this process and proposed methods of numerical simulation, mathematical

Received date: February 27, 2018

Foundation item: National Key Basic Research Development Program of China (2016YFB1100504); National Natural Science Foundation of China (51505301, 51375316); Shenyang Additive Manufacturing Engineering Research Center Program (F16-078-8-00)

Corresponding author: Yang Guang, Ph. D., Professor, Key Laboratory of Fundamental Science for National Defense of Aeronautical Digital Manufacturing Process, Shenyang Aerospace University, Shenyang 110136, P. R. China, Tel: 0086-24-89723852, E-mail: yangguang@sau.edu.cn

Copyright © 2019, Northwest Institute for Nonferrous Metal Research. Published by Science Press. All rights reserved.

modeling, real-time sensing and on-line control of the deposition process. Hussam et al^[11] developed two kinds of models to predict the form and the geometrical characteristics of the single laser tracks cross sections. The first model took into account the influence of powder distribution on the clad geometry, and the second model supposed that the general form of the clad cross section was a disk due to the surface tension forces. A two-input single-output controller was established to achieve stable layer growth by avoiding both over-building and compensating under-building by Song et al^[12], and the controller was successfully demonstrated to deposit a complex 3-D turbine blade. Smurov et al^[13] used a pyrometer to analyze variations of brightness temperature in the melt pool and a camera-based diagnostic tool to measure particle-in-fly velocity. And they studied two-phase jet flowing towards the substrate and particle focusing mechanism by numerical simulation. They observed that particle trajectories, temperature and averaged mass flow depend not only on the nozzle geometry but also on the type of particle collisions with the nozzle walls. Farahmand et al^[14] used Central Composite Design of experiments and Response Surface Methodology for the multi-objective optimization of the cladding process. And they presented that prediction of the geometry characteristics and mechanical properties could enhance the cladding characteristics, and both the processing time and raw material could be saved. Ding et al^[15] built a closed-loop control system consisting of a simple proportional integral derivation (PID) controller and feed-forward compensation. L-shaped single-bead walls built by this system achieved uniform bead width. Instead of using extensive designs of experiments, simulation could offer a chance to reduce times and costs. Thorsten et al^[16] developed a detailed energy absorption model which took various physics effects into consideration. They showed the significance of evaporation and its related recoil pressure for a feasible prediction of the melt pool dynamics.

Aim of this study is to determinate the correlations between melt pool width and parameters and to build a thin wall with uniform tracks geometry.

1 Experiment

1.1 Equipment and materials

In this study, the experiments were performed by a laser deposition manufacturing system established by the Key Laboratory of Fundamental Science for National Defense of Aeronautical Digital Manufacturing Process in Shenyang Aerospace University, which consists of a 3-axis worktable, a 6 kW fiber laser with a 1064 nm wavelength and a coaxial nozzle, as well as optical transmission equipments. The process parameters were controlled by metal powder manufacturing software. A high-speed CCD camera was fixed directly onto the laser head, and a self-developed image processing software was used to obtain melt pool size. Argon was used as both the powder carrier gas as well as the shielding gas to avoid any chemical

reaction with the injected powder. Fig.1 shows a schematic view of the deposition process and monitoring equipment.

The substrate material used in the experiments were annealed BT20 titanium alloy, and the metal powder was BT20 with a spherical shape and a diameter of 44~149 μm , and chemical compositions of the BT20 is listed in Table 1. The powder used was dried at 120 °C in a vacuum dryer and the substrate was polished and cleaned by acetone before LDM. The samples were cross sectioned vertical to the scanning direction by a wire electrical discharge machining (WEDM) and then polished and etched in an etchant containing 10 mL HF, 60 mL HNO₃ and 70 mL distilled water. The geometrical features of cross-sections in the center position were photographed by an optical microscope (OM).

1.2 Experimental design

To study correlations of the melt pool width and process parameters, single tracks in a length of 30 mm were built up in a wide variety of process parameters. A three-factors with five-levels (Table 2) orthogonal experimental design with 25 experimental trials were established. Using this method of experimental design could offer least possible number of experiments without losing accuracy. 25 tracks were carried out onto five substrates. Adjacent tracks were spacing 10 mm to avoid heat transfer between tracks (shown in Fig.2a).

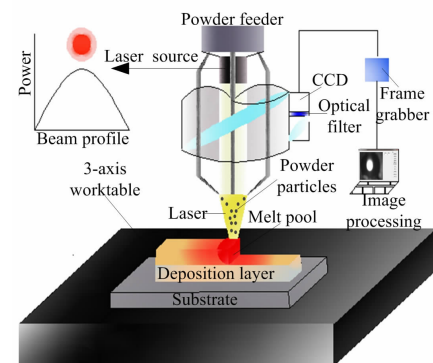


Fig.1 Schematic view of the deposition process and online monitoring

Table 1 Composition of BT20 titanium alloy (wt%)

Element	Content
Al	5.5~7.1
Zr	1.5~2.5
Mo	1.05~2.0
V	0.8~2.5
Ti	Bal.

Table 2 Parameters and their design levels

Parameter	Five level				
	1	2	3	4	5
Laser power, P/W	1400	1600	1800	2000	2200
Scanning speed, $V/\text{mm}\cdot\text{s}^{-1}$	7	9	11	13	15
Powder feeding rate, $Q_m/\text{g}\cdot\text{min}^{-1}$	3.2	5.1	7.2	9.1	11.1

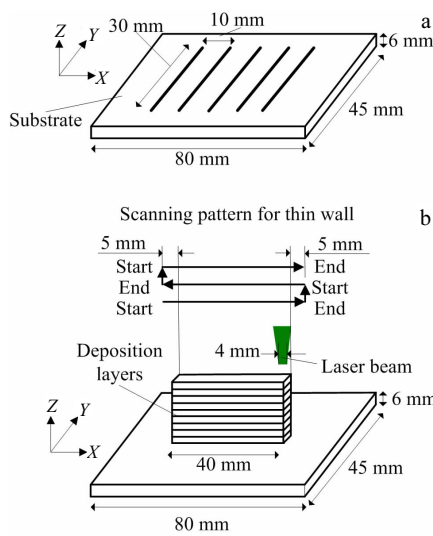


Fig.2 Single track deposition on the substrate (a) and thin wall and scanning pattern (b)

Moreover, two thin walls were built. Two cubic specimens with dimensions of 40 mm×4 mm×9 mm were built in a layer-by- layer fashion with 30 layers, the scanning pattern in Z direction is shown in Fig.2b. During the process, the laser head firstly moved 50 mm to one direction to build one layer, subsequently the laser head moved up in the Z direction for an increment with 0.3 mm, and then the laser head moved back to the original position to deposit the next layer. But the laser beam was off at the two ends (5 mm) of the track of the laser head. Other constant processing factors are listed in Table 3.

2 Melt Pool Width Modeling

LDM is a layer-by-layer process, so the width of each deposition layer governed by the melt pool width directly affects the forming geometry and accuracy of the final part. During the process, the melt pool width of each track changes with a number of parameters. Among these parameters, laser power, powder feeding rate, scanning speed and the beam diameter are typically significant. Due to the complexity of adjusting beam diameter randomly during the process, the melt pool width was modeled by the other three inputs. In this study, the parameters coefficients and empirical model for a single track based on multiple regression analysis were established in SPSS software.

The empirical model was firstly identified using linear regression model with the following form:

Table 3 Fixed processing parameters in the deposition process

Fixed parameter	Value
Shielding gas pressure/ $\times 10^2$ Pa	2.9
Flow powder transport gas pressure/Pa	400
Distance, nozzle-substrate/mm	13
Laser beam diameter/mm	4

$$D = c + \alpha P + \beta V + \gamma Q_m \quad (1)$$

where, D is the melt pool width (mm), P is the laser power (W), V is the scanning speed (mm/s), Q_m is the powder feeding rate (g/min), c is a constant, α , β and γ are coefficients of P , V and Q_m respectively. The stepwise regression method was used to eliminate the insignificant terms. And the level of confidence for developed model was considered to be 95%. With our experimental results, the melt pool width D was correlated to $0.001P-0.076V$ with a correlation coefficient $R= 0.92$ taking into account all the 25 experiments. The R value reflects the fit between predicted and measured data. The linear regression model demonstrates that the laser power has a linear positive effect on the melt pool width while scanning speed has a linear negative effect on the melt pool width. Also the powder feeding rate has a negligible influence on the melt pool width. The standard coefficient of the factor is used to compare the significance of various factors. Based on above analysis, the laser power has the most obvious effect on the melt pool width with a standard coefficient of 0.799 (the standard coefficient of scanning speed is -0.462). Nevertheless the R value was not big enough. In order to obtain a more persuasive relation, a nonlinear regression model was presented by Eq.(2):

$$D = K (P^\alpha V^\beta Q_m^\gamma) + c \quad (2)$$

where, K denotes the system gain, and c is a constant. With the experimental results, it could be found that D is proportional to $P^{0.467}V^{-0.165}$ with $R=0.94$. Based on ANOVA analysis (see Table 4) which is used to locate the significant effective process parameters for melt pool width, laser power is the most significant parameter associated to the melt pool width. And it is obvious that there is no association between powder feeding rate and the melt pool width. This is in agreement with the results of linear analysis.

The average relative error between the predicted and measured data was calculated by Eq.(3):

$$\bar{e} = \frac{1}{n} \sum_{i=1}^n \left| \frac{D_{\text{model}}(i) - D_{\text{measured}}(i)}{D_{\text{measured}}(i)} \right| \quad (3)$$

The predicted and measured data of melt pool width are shown in Fig.3, and plug them in Eq.(3), $\bar{e} = 3.5\%$. The results indicate that the melt pool width predicted by the empirical model matches the experimental data well. During the process, the melt pool image was captured by a CCD camera online with a sampling period of 0.04 s and then the melt pool width was

Table 4 ANOVA analysis for melt pool width

Source	Sums of squares	Degree of freedom	Mean square	F value	Significance level
Model	0.646	20	0.32		
P	3.555	4	0.887	35.297	0.000
V	1.485	4	0.371	14.770	0.000
Q_m	0.095	4	0.024	0.949	0.469
Pure error	0.302	12	0.025		
Total	366.7	25			

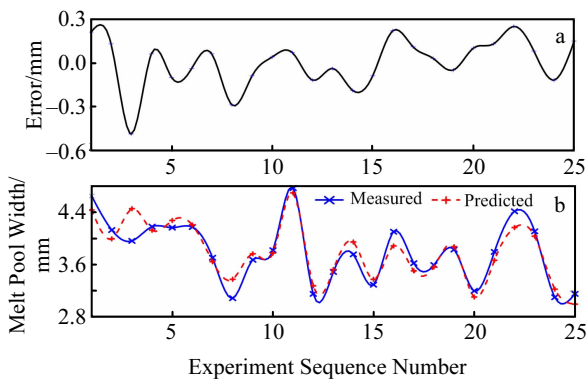


Fig.3 Relationship between measured and predicted melt pool width: (a) error between predicted and measured data and (b) predicted and measured data of melt pool width

obtained by image processing software. It should be noted that the measured melt pool width of each track are values averaged.

3 Result and Discussion

3.1 Kalman filter design

Normally, the measurement signals are contaminated by noises in equipment. In order to obtain true value of melt pool width, a first-order model Kalman filter (KF) algorithm was used. For this kind of filter algorithm, the solution is recursive in that each updated estimate of the state is computed from the previous estimate and the new input data^[17,18].

For the actualization of conventional Kalman filter model, the models of system equation and the observation equation should be known exactly. The Kalman filter gives a method for the recursive estimation of an unknown process x_t based on a known array y_t up to time t , the system equation and the observation equation are given as following:

$$x_t = kx_{t-1} + \omega_t \quad (4)$$

$$y_t = x_t + v_t \quad (5)$$

Where, x_t is the system state (i.e., melt pool width) at time t which denotes the discrete time step, y_t is the measurement value (i.e., measured melt pool width), k is the system pole, ω_t and v_t are system noise and measured noise, respectively. Also, both ω_t and v_t are white noise with zero mean. Based on the optimal value $x_{(t-1|t-1)}$ and $P_{(t-1|t-1)}$ at previous time step, a first estimate of $x_{(t|t)}$ and covariance $P_{(t|t)}$ are predicted by:

$$x_{(t|t-1)} = x_{(t-1|t-1)} \quad (6)$$

$$P_{(t|t-1)} = P_{(t-1|t-1)} + Q \quad (7)$$

Where, Q is the system covariance. As soon as the new observation value y_t is known, the estimate of the optimal value $x_{(t|t)}$ at time t becomes:

$$x_{(t|t)} = x_{(t|t-1)} + Kg_t [y_t - x_{(t|t-1)}] \quad (8)$$

Where,

$$Kg_t = P_{(t|t-1)} [P_{(t|t-1)} + R]^{-1} \quad (9)$$

Kg_t is Kalman gain, Kg_t arranges how easily the filter adjusts to possible new conditions. And R is covariance of the measured melt pool width. The final estimate of $P_{(t|t)}$ is

$$P_{(t|t)} = [1 - Kg_t] P_{(t|t-1)} \quad (10)$$

To illustrate the effect of the Kalman filter on the measured melt pool width signal, the filtered and measured melt pool width signal of the experiment conducted for KF validation are compared in Fig.4. The average relative error between filtered/measured melt pool width and predicted value was calculated by Eq.(11):

$$\bar{e}_{KF/Measured} = \frac{1}{n} \sum_{i=1}^n \left| \frac{D_{KF}(i) / D_{Measured}(i) - D_{Predicted}(i)}{D_{Predicted}(i)} \right| \quad (11)$$

After plugging the plots in Fig.4 into Eq.11 we obtain the results, $e_{KF} = 0.6\%$, $e_{Measured} = 1.4\%$. Apparently, the magnitude of the variation significantly decreases with the Kalman filter.

3.2 Process parameters significance

To validate the model in terms of the quantitative influence of the process parameters on the melt pool width, the single variable method was introduced to deposit nine more single tracks of 30 mm in length. As shown in Fig.5, the increase in the melt pool width reaches 3.57 mm increment (from 2.77 mm to 6.34 mm) for a triplication of the laser power from 800 W to 2400 W, which is an increase of 129%. Simultaneously, a decrease in the scanning speed from 15 mm/s to 5 mm/s leads to an enlargement of the melt pool size from 3.27 mm to 4.32 mm, which is an increase of 24%. Therefore the influence of the laser power on the melt pool width is much bigger in comparison to the influence of the scanning speed. Besides, the melt pool width is hardly affected by the increase of the powder feeding rate. The experimental results match the predicted results well.

Fig.6 shows the melt pool image of 25 single tracks in the center position of each track. The correlation between the scanning speed and melt pool width is negative. If the laser power remains constant, the melt pool width decreases slightly with the increase of scanning speed. On the other hand,

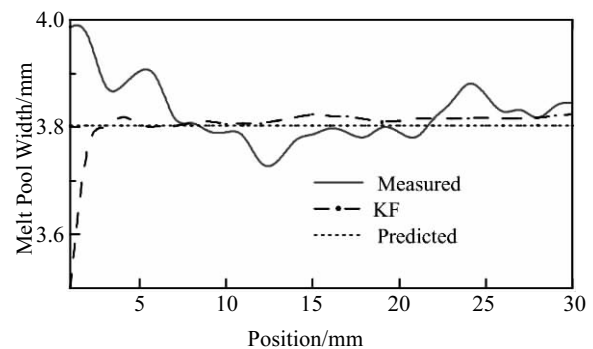


Fig.4 Plots of measured, modeled and filtered melt pool width using KF ($P=1800$ W, $V=11$ mm/s, $Q_m=3.26$ g/min)

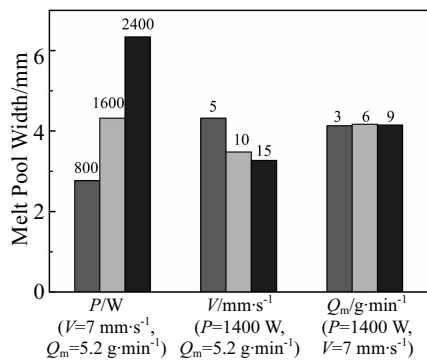


Fig.5 Melt pool width for different process parameters

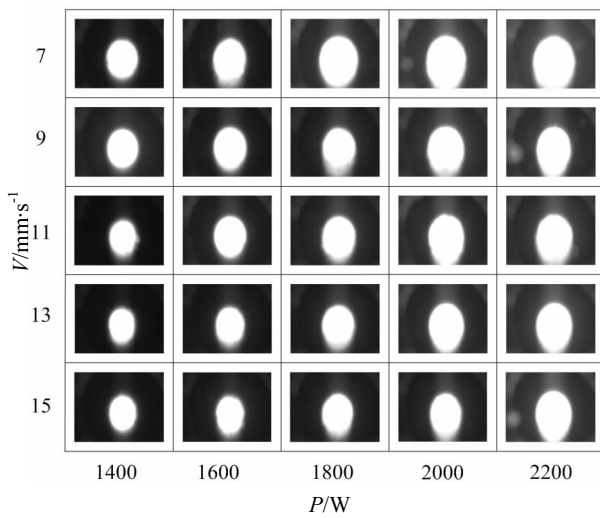


Fig.6 All single tracks' melt pool in the center position of the track

keeping the scanning speed either at lower or higher level and increasing the laser power at the same time could lead to the maximum melt pool width. This result could be explained by the fact that the melt pool width is controlled by a thermal effect which depends directly on the laser power.

The effect of interaction between laser power and scanning speed on the melt pool width are plotted in Fig.7. As it is seen in Fig.7b, even if the range of variation of process parameters is very large, the average melt pool width is rather stable: the melt pool width fluctuates within a certain range from the spot diameter which is a constant value of 4 mm during each experiment. The process parameters combination could be divided into three regions, namely, region A, B and C. Two single tracks were selected in each region to analyze their geometrical characteristics. For a much lower laser power (region A, Fig.7b), the melt pool width is smaller (track 1 and track 2, Fig.8). And fixed processing parameters for six tracks are shown in Table 5.

On the other hand, for a high laser power combined with a low scanning speed (region C, Fig.7b), the melt pool width is bigger (track 5 and track 6, Fig.8). A combination of a

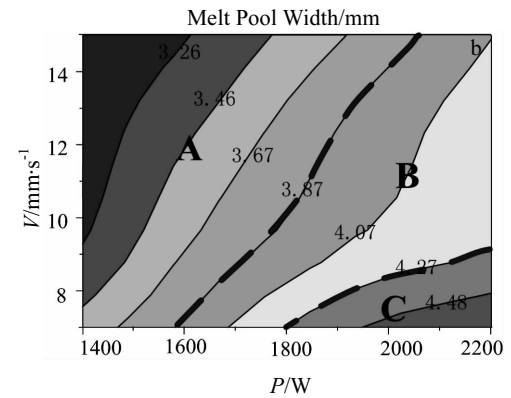
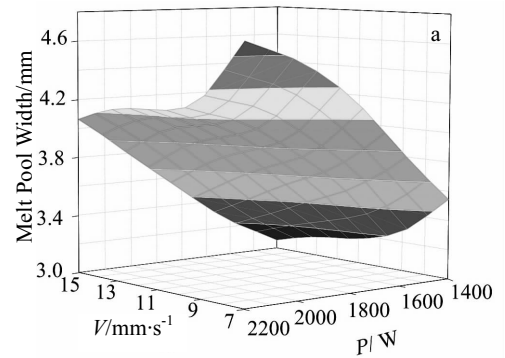


Fig.7 Interaction effect of laser power and scanning speed on melt pool width: (a) 3D surface plot and (b) isothermal graph

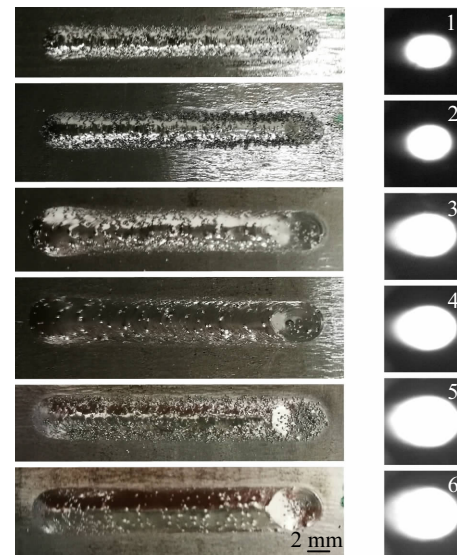


Fig.8 Single tracks and their corresponding melt pool

sufficiently high laser power and a reasonable scanning speed (region B, Fig.7b) could generate an appropriate melt pool width and guarantee sufficient melting of the captured powder and achieve a single track with good geometrical characteristics (track 3 and track 4, Fig.8).

Table 5 Fixed processing parameters in the deposition process

Track No.	P/W	V/mm·s ⁻¹	Q _m /g·min ⁻¹	D/mm
1	1400	11	1.1	3.11
2	1400	13	1.4	3.21
3	2200	9	1.1	3.97
4	2000	13	0.5	4.11
5	2000	7	1.1	4.65
6	2200	7	0.8	4.77

3.3 Thin-wall process control

A perfect LDM system should be able to deposit a part with any desired width either uniform or non-uniform. For a thin wall deposited with fixed process parameters, the width of the layer shows an obvious increase as the wall grows (Fig.9). This mushroom effect correlates to the heat accumulation in the component with limited heat conductivity during the LDM process, which will make the rise of the melt pool width in the vertical direction.

During LDM process, the spot size, the powder feeding rate and the scanning speed were constant of 4 mm, 5.2 g/min and 7 mm/s, respectively. The experiment was firstly carried out with a constant laser power of 1400 W. And the mean value of melt pool width was calculated for each layer. Then a thin wall with adapted laser power was built up, and the adapted laser power values of each layer was estimated via the particle swarm optimization (PSO) algorithm based on the results with the fixed laser power of 1400 W.

Let *N* be the number of particles in *D*-dimensional space, each having a position *X_i* and a velocity *V_i*. Let *Pbest_i* be the individual extreme and let *gbest_i* be the global extreme. The classic PSO algorithm steps are as follows^[19,20]: First, initialize particles with random position and velocity vector and then evaluate the fitness for each particle's position. After several iterative cycles, particle's position and velocity are updated and recorded. When all the iteration is completed, the optimal position is received.

In classic PSO, the update formula of particle's velocity is

$$V'_m = \omega_i V^{t-1}_m + c_1 rand_1(\dots)(Pbest_m - X^{t-1}_m) + c_2 rand_2(\dots)(gbest_m - X^{t-1}_m) \tag{12}$$

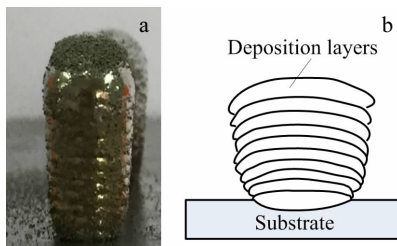


Fig.9 Thin wall deposited by constant process parameters (a) and deposition model for a thin-walled cross section (b)

And the update formula of particle's location is

$$X^t_m = X^{t-1}_m + V^t_m \tag{13}$$

Among them, *c₁* is cognitive acceleration constant and *c₂* is social acceleration constant, *rand₁* and *rand₂* are random number between 0 and 1, *n* represents the problem dimension ($1 \leq n \leq N$), *ω* means inertia weight value and is mathematically defined as:

$$\omega_t = \omega_{max} - \frac{\omega_{max} - \omega_{min}}{T} \cdot t \tag{14}$$

where *t* is current iteration, and *T* is total number of iterations. The fitness function which is significant for the optimization results is built based on the empirical model (Eq.(3)) and expresses by Eq.(15):

$$F = \omega_n |D_1 - \hat{D}_1| \tag{15}$$

And the prediction model of the process parameters for the LDM process of a thin wall is expressed as Eq.(16):

$$\text{Min}(D - \hat{D}) = \text{Min} \left[K(P^\alpha V^\beta) + c - \hat{D} \right] \tag{16}$$

where *Ď₁* is the expected value for melt pool width, and Min means the minimum value. To run the PSO algorithm, the related control parameters are selected as bellows:

Number of particles is 40, maximum iteration number is 100, *ω_{max}*=0.9, *ω_{min}*=0.4, weighting factor *c₁*=*c₂*=2. *D*=4 mm, 800 W ≤ *P* ≤ 2400 W.

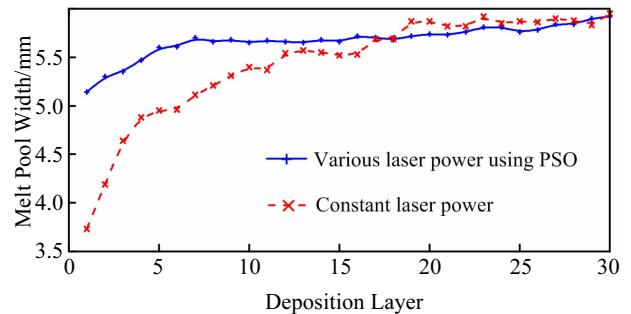


Fig.10 Melt pool width of thin wall with constant and adapted laser power during deposition

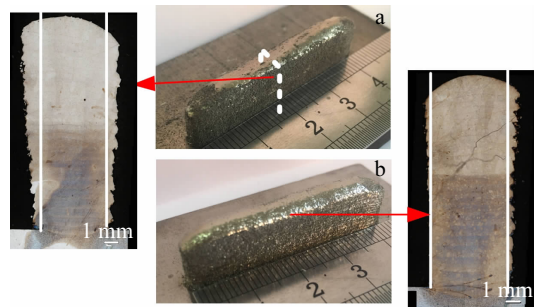


Fig.11 Thin wall and vertical cross-section of buildup: (a) with constant process parameters and (b) with process parameters estimated by PSO

Laser power for each deposition layer was estimated by the PSO algorithm. An experiment with adapted laser power values was then performed. However, the melt pool width was much more stable than that with constant laser power as the thin wall grows gradually (Fig.10). And a thin wall with uniform layer width could be formed by using adapted laser power (shown in Fig.11).

4 Conclusions

1) Kalman filter is found to be significantly smooth measured signals and obtain more accurate melt pool width information.

2) The variation of the melt pool width is more pronounced by changing the laser power than scanning speed. And powder feeding rate has insignificant influence on melt pool width. The predicted results based on developed analytical model are in good agreement with the actual measured results.

3) Too small or too large melt pool width will both deteriorate the geometrical characteristics of the single track. A sufficiently high laser power with a reasonable scanning speed could generate an appropriate melt pool width and guarantee sufficient melting of the captured powder.

4) Compared with the thin wall deposited by constant process parameters, the inconsistent track width could be eliminated significantly by using adapted laser power.

References

- 1 Elwany A, Tapia G. *Manufacturing Science and Engineering*[J], 2014, 136(6): 60 801
- 2 Shi Qimin, Gu Dongdong, Xia Mujianl et al. *Optics & Laser Technology*[J], 2016, 84: 9
- 3 Zhong Chongliang, Gasser A, Kittel J. *Material and Design*[J], 2016, 98: 128
- 4 Ravi G A, Hao X J, Wain N. *Materials and Design*[J], 2013, 47: 731
- 5 De A, Debroy T. *Journal of Applied Physics*[J], 2014, 116: 1 249 051
- 6 Yu Jun, Lin Xin, Chen Junjie et al. *Applied Surface Science*[J], 2010, 256: 4612
- 7 Wang T, Zhu Y Y, Zhang S Q et al. *Journal of Alloys and Compounds*[J], 2015, 632: 505
- 8 Lu Yuanhang, Yuan Linjiang, Cai Dingdao et al. *Rare Metal Materials and Engineering*[J], 2014, 43(10): 2349
- 9 Qiu Chunlei, Ravi G A, Dance C. *Journal of Alloys and Compounds*[J], 2015, 692: 351
- 10 Farahmand P, Liu Shuang, Zheng Zhe et al. *Ceramics International*[J], 2014, 40(10): 15 421
- 11 Hussam E C, Bruno C, Samuel B. *Optics and Lasers in Engineering*[J], 2012, 50(3): 413
- 12 Song Lijun, Vijayavel B S, Dutta B. *Int J Adv Manuf Technol*[J], 2012, 58(1): 247
- 13 Smurov I, Doubenskaia M, Zaitsev A. *Physics Procedia*[J], 2012, 39: 743
- 14 Farahmand P, Kovacevic R. *Lasers in Manufacturing & Materials Processing*[J], 2014, 1: 1
- 15 Ding Yaoyu, Warton J, Kovacevic R. *Additive Manufacturing*[J], 2016, 10: 24
- 16 Thorsten H, Mechael C, Konrad W et al. *Additive Manufacturing*[J], 2017, 14: 116
- 17 Lie Tang, Robert G. *Journal of Manufacturing Science and Engineering*[J], 2010, 132: 11 010
- 18 Ahmad M, Alireza F, Amir K. *Applied Soft Computing*[J], 2013, 13: 1505
- 19 Ji Weidong, Zhu Songyu. *International Journal of U-and E-Service, Science and Technology*[J], 2016, 9(1): 179
- 20 Kennedy J, Eberhart R C. *Proceedings of the IEEE International Conference on Networks*[J], 1995, 4(8): 1942

基于熔池监测的激光沉积制造成形工艺参数的分析及预测

钦兰云, 徐丽丽, 杨光, 尚纯, 王维

(沈阳航空航天大学 航空制造工艺数字化国防重点学科实验室, 辽宁 沈阳 110136)

摘要: 激光沉积制造 (LDM) 过程中, 熔池宽度是成形精度的关键, 主要受到工艺参数的影响。本文建立了基于 CCD 高速摄像机的熔池在线监测系统。为了提高熔池宽度检测精度, 应用卡尔曼滤波技术对熔池宽度测量值进行了去噪处理。采用正交实验设计方法和多元回归分析, 建立了熔池宽度与 3 个主要工艺参数 (激光功率、扫描速度和送粉速率) 间的关系模型。并设计单一变量实验对模型进行了验证。最后, 利用粒子群算法 (PSO) 对薄壁结构的成形过程参数进行了预测。结果表明, 对 LDM 成形过程进行工艺参数的分析和预测为实现沉积层成形精度的控制提供了依据。

关键词: 激光沉积制造; 熔池; 粒子群优化; 关系模型; 卡尔曼滤波

作者简介: 钦兰云, 女, 1977 年生, 博士, 副教授, 沈阳航空航天大学航空制造工艺数字化国防重点学科实验室, 辽宁 沈阳 110136, 电话: 024-89723852, E-mail: qinly@sau.edu.cn